Structural Engineering and Mechanics, *Vol. 70, No. 5 (2019) 551-562*
DOI: https://doi.org/10.12989/sem.2019.70.5.551

Transient response of rhombic laminates

Anish[1], Abhay K. Chaubey[2], Satyam Vishwakarma[3], Ajay Kumar*[3], Stanisław Fic[4] and Danuta Barnat-Hunek[4]

[1]*Department of Civil Engineering, Birla Institute of Technology Mesra, Patna Camus, Patna - 800014, India*
[2]*Department of Civil Engineering, Koneru Lakshmaiah Education Foundation, Vaddeswaram 522502, India*
[3]*Department of Civil Engineering, National Institute of Technology Patna, Patna-800005, India*
[4]*Department of Construction, Faculty of Civil Engineering and Architecture, Lublin University of Technology, Nadbystrzycka 40, Lublin, Poland*

(Received September 10, 2018, Revised March 5, 2019, Accepted March 8, 2019)

Abstract. In the present study, a suitable mathematical model considering parabolic transverse shear strains for dynamic analysis of laminated composite skew plates under different types of impulse and spatial loads was presented for the first time. The proposed mathematical model satisfies zero transverse shear strain at the top and bottom of the plate. On the basis of the cubic variation of thickness coordinate in in-plane displacement fields of the present mathematical model, a 2D finite element (FE) model was developed including skew transformations in the mathematical model. No shear correction factor is required in the present formulation and damping effect was also incorporated. This is the first FE implementation considering a cubic variation of thickness coordinate in in-plane displacement fields including skew transformations to solve the forced vibration problem of composite skew plates. The effect of transverse shear and rotary inertia was incorporated in the present model. The Newmark-β scheme was adapted to perform time integration from step to step. The C^0 FE formulation was implemented to overcome the problem of C^1 continuity associated with the cubic variation of thickness coordinate in in-plane displacement fields. The numerical studies showed that the present 2D FE model predicts the result close to the analytical results. Many new results varying different parameter such as skew angles, boundary conditions, etc. were presented.

Keywords: transient analysis; laminated composite skew plate; impulse

1. Introduction

Composites are becoming an alternative material to be used extensively in construction or fabrication for high performance and reliability applications. Laminated composite plates have been extensively used in many engineering applications due to their properties of high strength to weight ratio and excellent corrosion resistance. When manufacturing a composite material, the material and structure are often made in single process. There are various methods of manufacture of laminated composites (Campbell 2003). Due to the wide application of the laminated composite material in various engineering fields, it becomes vital to perform a numerical analysis to use the obtained results in the structural design process. This situation has led to the development of efficient and accurate numerical analysis techniques, required to predict the behaviour of laminated plates.

Chamis (2006) developed the results of the vibration analysis for the laminated composite structures, as the study aimed upon the resonant behaviour of the structures. Moreover, most structures, whether used in civil, marine or aerospace applications, are often subjected to dynamic loads during their operation, and therefore assessing the dynamic response of laminated composites is required. Still, the dynamic analyses for laminated composite plates of finite dimensions have not received enough attention. Many researchers proposed different results on the transient response of laminated composite plates.

Sun and Whitney (1974) performed a transient analysis of an infinitely long simply supported composite plate subjected to uniform or line concentrated dynamic load at the upper surface of the plate. Different types of pulse-like rectangular, triangular, sinusoidal and dynamic load factor were applied to determine the maximum value of deflection, bending stress. Reddy (1983) employed the shear flexible element that was stable and accurate to predict the dynamic response of laminate composites. The analysis used the Newmark direct integration technique to perform transient response of isotropic, orthotropic and layered anisotropic composite plates to generate the results for deflection and stress for rectangular plates under various boundary conditions and loadings.

Mallikarjuna and Kant (1988) used simple C^0 isoparametric formulation of an assumed higher-order displacement model that was stable and accurate in predicting the transient response of composite plates. Kant *et al*. (1992) applied refined shear deformation theory and mode superposition technique for evaluating the transient response which was found to be very effective for the linear dynamic response for symmetric and non-symmetric composite plates. Hoa and Xiao (1998) developed a rectangular plate bending element based on higher order

*Corresponding author, Assistant Professor
E-mail: sajaydce@gmail.com

ISSN: 1225-4568 (Print), 1598-6217 (Online)

shear deformation theory having four nodes and twenty degrees of freedom at each node. (Wang *et al*. 2001) used classical laminate plate theory and developed the strip element method to analyze the transient behaviour of the symmetric rectangular laminated composite plates. The results obtained had a different type of boundary conditions. Ahmadian and Zangeneh (2003) analysed the dynamic behaviour of the rectangular composite plates using a four-noded super element to obtain the transient responses. The transient flexural response analysis of anisotropic laminated composite plates of bi-modulus materials subjected to mechanical loading was carried out by Patel *et al*. (2005). Shooshtari and Khadem (2006) studied the free and forced vibration of rectangular plates using Galerkin method. Kiral and Kiral (2008) used the FE method and the Newmark integration method to calculate the dynamic responses. Tahani and Torghabeh (2011) used layerwise theory to analyse the dynamic response of a thick cross-ply laminated plate. The dynamic analyses for a fixed-fixed sandwich and laminated composite plate under the action of a moving load were carried out by Mantari *et al*. (2012) using a new higher order shear deformation theory. Yousefi *et al*. (2012) used Hertz contact theory to analyse the dynamic responses of the composite plates. Dambal and Sharma (2013) obtained results for composite plates under dynamic loading in form of half sine wave. Ahmed *et al*. (2013) and Maithry *et al*. (2012) used first-order shear deformation theory to analyse the transient response of composite plates for varied layer orientation and aspect ratio. Lee and Kim (2013) analysed the dynamic behaviour of the laminated composite plate using a new higher order shear deformation theory. A four-noded element was considered having seven degrees of freedom at each node. Adim *et al*. (2016) used a refined higher order shear deformation theory of plates. Forced vibration of the elastic system is studied by Akbarov and Mehdiyev (2017) using a mathematical formulation of the exact equations of linear elastodynamics. Golewski (2017, 2018a, 2018b) has investigated behavior of concrete composites using experimental procedure.

From the above-mentioned literature review, it is observed that there is no work on the dynamic analysis of laminated composite skew plate using improved shear deformation theory. Most of these studies were based upon FSDT and HSDT and that too for laminated composite plate without skew effects. Hence, in the present work, an attempt has been made to analyse the laminated composite skew plate under different types of spatial and transient loads.

2. ISDT (Improved Shear Deformation Theory)

In the present deformation theory, the transverse shear stresses at the top and bottom of the laminate were taken as zero. It was assumed that variation of transverse shear strains was realistic parabolic in shape and the use of shear correction factor was hence avoided. The present theory consists of a realistic cubic variation of in-plane displacement fields.

For the present analysis, the following equation for displacement fields was adopted

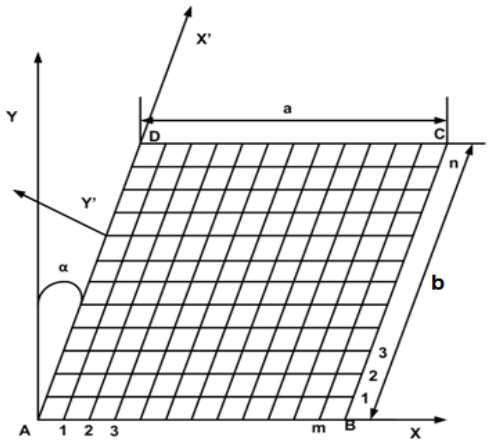

Fig. 1 Laminated composite plate

$$\begin{Bmatrix} u \\ v \\ w \end{Bmatrix} = \begin{Bmatrix} u_0 \\ v_0 \\ w_0 \end{Bmatrix} + z\begin{Bmatrix} \theta_x \\ \theta_y \\ 0 \end{Bmatrix} + z^2\begin{Bmatrix} \xi_x \\ \xi_y \\ 0 \end{Bmatrix} + z^3\begin{Bmatrix} \zeta_x \\ \zeta_y \\ 0 \end{Bmatrix} \tag{1}$$

In the equation above, u, v and w represent the displacements of a point along the three directions (x, y, and z as shown in Fig 1.) respectively, whereas it's associated midplane displacements are given by u_0, v_0, and w_0 respectively. θ_x and θ_y signify the rotations of transverse normal in the x–z and y–z planes, respectively.

ζ_x, ζ_x, ζ_y and ζ_y functions in the equations above were determined using an assumption of zero transverse shear strains at the top and bottom surfaces of the plate i.e.

$$\gamma_{xz}(x,\ y, \pm h/2) \text{ and } \gamma_{yz}\ (x,\ y, \pm h/2)\ = 0 \tag{2}$$

Since,

$$\gamma_{xz} = \frac{\partial u}{\partial z} + \frac{\partial w}{\partial x} \text{ and } \gamma_{yz} = \frac{\partial v}{\partial z} + \frac{\partial w}{\partial y}$$

So,

$$\gamma_{xz} = \theta_x + 2z\xi_x + 3z^2\zeta_x + \frac{\partial w}{\partial x}$$

$$\text{And} \quad \gamma_{yz} = \theta_y + 2z\xi_y + 3z^2\zeta_y + \frac{\partial w}{\partial y} \tag{3}$$

Using Eqs. (2) - (3), we get

$$\xi_x = 0 \text{ and } \xi_y = 0$$

$$\zeta_x = -\frac{4}{3h^2}(\theta_x + \frac{\partial w}{\partial x}) \text{ and } \zeta_y = -\frac{4}{3h^2}(\theta_y + \frac{\partial w}{\partial y}) \tag{4}$$

When replaced, the values obtained in Eq. (4) to Eq. (1), are:

$$\begin{Bmatrix} u \\ v \\ w \end{Bmatrix} = \begin{Bmatrix} u_0 \\ v_0 \\ w_0 \end{Bmatrix} + z(1-4z^2/3h^2)\begin{Bmatrix} \theta_x \\ \theta_y \\ 0 \end{Bmatrix} - 4z^3/3h^2\begin{Bmatrix} \partial w_0/\partial x \\ \partial w_0/\partial y \\ 0 \end{Bmatrix} \tag{5}$$

or,

$$\begin{Bmatrix} u \\ v \\ w \end{Bmatrix} = \begin{Bmatrix} u_0 \\ v_0 \\ w_0 \end{Bmatrix} + z(1-4z^2/3h^2)\begin{Bmatrix} \theta_x \\ \theta_y \\ 0 \end{Bmatrix} - 4z^3/3h^2 \begin{Bmatrix} \psi_x^* \\ \psi_y^* \\ 0 \end{Bmatrix}$$

The linear strains may be represented in the form of linear displacement:

$$\begin{Bmatrix} \varepsilon_x \\ \varepsilon_y \\ \gamma_{xy} \\ \gamma_{xz} \\ \gamma_{yz} \end{Bmatrix} = \begin{Bmatrix} \partial u/\partial x \\ \partial v/\partial y \\ \partial u/\partial y + \partial v/\partial x \\ \partial u/\partial z + \partial w/\partial x \\ \partial v/\partial z + \partial w/\partial y \end{Bmatrix} \tag{6}$$

Using the values of displacements from Eq. (5) - (6), the following equation is obtained,

$$\begin{Bmatrix} \varepsilon_x \\ \varepsilon_y \\ \gamma_{xy} \\ \gamma_{xz} \\ \gamma_{yz} \end{Bmatrix} = \begin{Bmatrix} \partial u_0/\partial x \\ \partial v_0/\partial y \\ \partial u_0/\partial y + \partial v_0/\partial x \\ \partial w_0/\partial x + \theta_x \\ \partial w_0/\partial y + \theta_y \end{Bmatrix} + z(1-4z^2/3h^2)\begin{Bmatrix} \partial\theta_x/\partial x \\ \partial\theta_y/\partial y \\ \partial\theta_x/\partial y + \partial\theta_y/\partial x \\ 0 \\ 0 \end{Bmatrix}$$
$$-\frac{4z^3}{3h^2}\begin{Bmatrix} \partial\psi_x^*/\partial x \\ \partial\psi_y^*/\partial y \\ \partial\psi_x^*/\partial y + \partial\psi_y^*/\partial x \\ 0 \\ 0 \end{Bmatrix} - \frac{12z^2}{3h^2}\begin{Bmatrix} 0 \\ 0 \\ 0 \\ \theta_x + \psi_x^* \\ \theta_y + \psi_y^* \end{Bmatrix} \tag{7}$$

Or

$$\begin{Bmatrix} \varepsilon_x \\ \varepsilon_y \\ \gamma_{xy} \\ \gamma_{xz} \\ \gamma_{yz} \end{Bmatrix} = \begin{Bmatrix} \varepsilon_{x0} \\ \varepsilon_{y0} \\ \gamma_{xy0} \\ \phi_x \\ \phi_y \end{Bmatrix} + z(1-4z^2/3h^2)\begin{Bmatrix} K_x \\ K_y \\ K_{xy} \\ K_{xz} \\ K_{yz} \end{Bmatrix} - \frac{4z^3}{3h^2}\begin{Bmatrix} K^*_x \\ K^*_y \\ K^*_{xy} \\ K^*_{xz} \\ K^*_{yz} \end{Bmatrix} - \frac{12z^2}{3h^2}\begin{Bmatrix} K^{**}_x \\ K^{**}_y \\ K^{**}_{xy} \\ K^{**}_{xz} \\ K^{**}_{yz} \end{Bmatrix} \tag{8}$$

The strains associated with Eq. (8) are related to the generalized strains by means of the following expression:

$$\{\bar{\varepsilon}\} = [H]\{\varepsilon\} \tag{9}$$

where

$$\{\bar{\varepsilon}\} = \begin{bmatrix} \varepsilon_x \varepsilon_y \gamma_{xy} \gamma_{xz} \gamma_{yz} \end{bmatrix}^T$$

and

$$\{\varepsilon\} = \begin{Bmatrix} \varepsilon_{x0}, \kappa_x, \kappa_x^*, \gamma_{x0}, \varepsilon_{y0}, \kappa_y, \kappa_y^*, \gamma_{y0}, \\ \kappa_{xy}, \kappa_{xy}^*, w_0, \theta_x, \psi_x, v_0, \theta_y, \psi_y, u_0 \end{Bmatrix}^T$$

$\{\varepsilon\}$ is the function of x and y and $[H]$ is the function of thickness coordinate z.

Further, the strain vector $\{\varepsilon\}$ can be interrelated with displacement vector $\{X\}$ by means of the following relationship.

$$\{\varepsilon\} = [B]\{X\} \tag{10}$$

where

$$\{X\} = \{u_0, v_0, w_0, \theta_x, \theta_y, \psi_x, \psi_y\}$$

For typical lamina (k^{th}), the constitutive relations with respect to the material axis can be expressed as.

$$\{\sigma\}_k = [Q]_k \{\varepsilon\}_k$$

i.e.

$$\begin{Bmatrix} \sigma_1 \\ \sigma_2 \\ \tau_{12} \\ \tau_{13} \\ \tau_{23} \end{Bmatrix}_k = \begin{bmatrix} Q_{11} & Q_{12} & 0 & 0 & 0 \\ Q_{12} & Q_{22} & 0 & 0 & 0 \\ 0 & 0 & Q_{66} & 0 & 0 \\ 0 & 0 & 0 & Q_{44} & 0 \\ 0 & 0 & 0 & 0 & Q_{55} \end{bmatrix}_k \begin{Bmatrix} \varepsilon_1 \\ \varepsilon_2 \\ \gamma_{12} \\ \gamma_{13} \\ \gamma_{23} \end{Bmatrix}_k \tag{11}$$

where,

$$\frac{\upsilon_{12}}{E_1} = \frac{\upsilon_{21}}{E_2}$$

and

$$\begin{bmatrix} Q_{11} & Q_{12} & 0 & 0 & 0 \\ Q_{12} & Q_{22} & 0 & 0 & 0 \\ 0 & 0 & Q_{66} & 0 & 0 \\ 0 & 0 & 0 & Q_{44} & 0 \\ 0 & 0 & 0 & 0 & Q_{55} \end{bmatrix}_k$$
$$= \begin{bmatrix} E_1/1-\nu_{12}\nu_{21} & \nu_{12}E_2/1-\nu_{12}\nu_{21} & 0 & 0 & 0 \\ \nu_{12}E_2/1-\nu_{12}\nu_{21} & E_2/1-\nu_{12}\nu_{21} & 0 & 0 & 0 \\ 0 & 0 & G_{12} & 0 & 0 \\ 0 & 0 & 0 & G_{13} & 0 \\ 0 & 0 & 0 & 0 & G_{23} \end{bmatrix}_k$$

The stress-strain relationship with respect to global coordinate axis system (x, y, and z) for k^{th} lamina can be expressed as shown below using transformation coefficients:

$$\begin{Bmatrix} \sigma_x \\ \sigma_y \\ \tau_{xy} \\ \tau_{xz} \\ \tau_{yz} \end{Bmatrix}_k = \begin{bmatrix} \bar{Q}_{11} & \bar{Q}_{12} & 0 & 0 & 0 \\ \bar{Q}_{12} & \bar{Q}_{22} & 0 & 0 & 0 \\ 0 & 0 & \bar{Q}_{66} & 0 & 0 \\ 0 & 0 & 0 & \bar{Q}_{44} & 0 \\ 0 & 0 & 0 & 0 & \bar{Q}_{55} \end{bmatrix}_k \begin{Bmatrix} \varepsilon_x \\ \varepsilon_y \\ \varepsilon_{xy} \\ \gamma_{xz} \\ \gamma_{yz} \end{Bmatrix}_k \tag{12}$$

Integration of the stresses through the laminate thickness will help in obtaining the resultant forces and moments acting on the laminate, which is as follows:

$$[M] = \begin{bmatrix} M_x & M^*_x \\ M_y & M^*_y \\ M_{xy} & M^*_{xy} \end{bmatrix} = \sum_{K=1}^{N_L} \int_{Z_K}^{Z_{K+1}} \begin{bmatrix} \sigma_x \\ \sigma_y \\ \tau_{xy} \end{bmatrix} \begin{bmatrix} z, z^3 \end{bmatrix} dz \text{ and}$$
$$[N] = \begin{bmatrix} N_x \\ N_y \\ N_{xy} \end{bmatrix} = \sum_{K=1}^{N_L} \int_{Z_K}^{Z_{K+1}} \begin{bmatrix} \sigma_x \\ \sigma_y \\ \tau_{xy} \end{bmatrix} dz \tag{13}$$

$$\left[Q,S,S^{*},S^{**}\right]=\begin{bmatrix}Q_x & S_x & S_x^{*} & S_x^{**}\\ Q_y & S_y & S_y^{*} & S_y^{**}\end{bmatrix}$$

$$=\sum_{K=1}^{N_L}\int_{Z_K}^{Z_{K+1}}\begin{bmatrix}\tau_{xz}\\ \tau_{yz}\end{bmatrix}\left[1,z,z^2,z^3\right]dz$$

$$\text{or,}\quad \left\{\bar{\sigma}\right\}=\left[\bar{D}\right]\left\{\bar{\varepsilon}\right\}$$

where

$$\left\{\bar{\sigma}\right\}=\begin{bmatrix}N_x,N_y,N_{xy},\mathrm{M}_x,\mathrm{M}_y,\mathrm{M}_{xy},\mathrm{M}_x^{*},\mathrm{M}_y^{*},\mathrm{M}_{xy}^{*}\\ \theta_x,\theta_y,\mathrm{S}_x,\mathrm{S}_y,\mathrm{S}_x^{*},\mathrm{S}_y^{*},\mathrm{S}_x^{**},\mathrm{S}_y^{**}\end{bmatrix}^T,$$

$$\left\{\bar{\varepsilon}\right\}=\begin{bmatrix}\varepsilon_{x0},\varepsilon_{y0},\gamma_{xy0},\mathrm{K}_x,\mathrm{K}_y,\mathrm{K}_{xy},\mathrm{K}_x^{*},\mathrm{K}_y^{*},\mathrm{K}_{xy}^{*},\\ \phi_x,\phi_y,\mathrm{K}_{xz},\mathrm{K}_{yz},\mathrm{K}_{xz}^{*},\mathrm{K}_{yz}^{*},\mathrm{K}_{xz}^{**},\mathrm{K}_{yz}^{**}\end{bmatrix}^T$$

And the size of the [$\bar{\mathrm{D}}$] (rigidity matrix) is 17 x 17.

Thus, by following the standard procedure of FEM, the element matrices were assembled which results in global stiffness matrices i.e. [K] and [M].

2.1 Finite element formulation

The finite element formulation involved in the above-mentioned theories is as follows:

In the present study, the proposed finite element model uses C^0 isoparametric elements having nine nodes. The proposed element has seven unknowns at each node i.e. u_1, u_2, u_3, Ψ_1, Ψ_2, w_1 and w_2 (Fig. 2). The generalized displacements included in the present theory can be expressed as follows.

$$u_1=\sum_{i=1}^{9}N_iu_i;\ u_2=\sum_{i=1}^{9}N_iv_i;\ u_3=\sum_{i=1}^{9}N_iw_i;\ \psi_1$$
$$=\sum_{i=1}^{9}N_i\psi_{1i};\ \psi_2=\sum_{i=1}^{9}N_i\psi_{2i};\qquad(14)$$
$$w_1=\sum_{i=1}^{9}N_iw_{1i};\ w_2=\sum_{i=1}^{9}N_iw_{2i}$$

Where, N_i represents the related node's shape function.

Knowing the nodal unknown vector within an element helps to express the mid-surface strains at any point in the plate in the matrix form, in terms of global displacements, as shown below:

$$\left\{\bar{\varepsilon}\right\}=\sum_{i=1}^{9}\left[B_i\right]\left\{d_i\right\}\qquad(15)$$

Where [B_i]: is the matrix containing the differential operator of the shape function.

For an element, the element stiffness matrix (say, e^{th}), including the transverse shear effects, flexure and membrane can be given as:

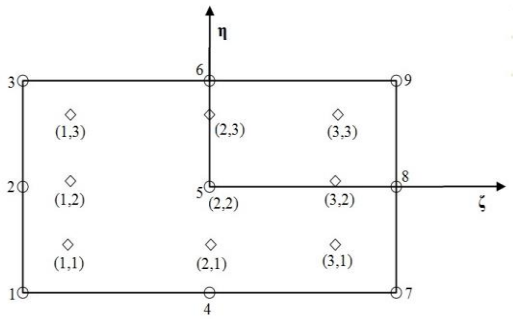

Fig 2. Nine-noded isoparametric element with typical node numbering and gauss points

$$\left[K_e\right]=\int_{-1}^{1}\int_{-1}^{1}[B]^T[D][B]|J|drds\qquad(16)$$

$$\left[M_e\right]=\int_{-1}^{1}\int_{-1}^{1}[N]^T[\rho][N]|J|drds\qquad(17)$$

In the equations above, [N] represents the matrix of shape function, [ρ] inertia matrix and |J| represents the determinant of a Jacobian matrix.

A 3 x 3 Gaussian Quadrature format was used for all numerical integrations. Then, using the characteristic procedures of the FE method by (Bathe 1996), the global stiffness matrices [K] was achieved by assembling the element matrices together.

The C^0 FE formulation, even though being a 2D solution, yielded the results closer to the closed form of solutions. Thus, the complexities of the solutions involved were reduced.

The element stiffness and mass matrix were evaluated and assembled together to form the global stiffness matrix [$\mathrm{K_g}$] and mass matrix [$\mathrm{M_g}$]

$$\left[C_g\right]=\alpha\left[M_g\right]+\beta\left[K_g\right]\qquad(18)$$

[C_g]: Global damping matrix

α and β: Rayleigh's proportionality constant was evaluated by solving for any two free vibration frequencies (ζ_m and ζ_n)

$$\begin{Bmatrix}\alpha\\ \beta\end{Bmatrix}=\frac{2\omega_m\omega_n}{\omega_n^2-\omega_m^2}\begin{pmatrix}\omega_n & \omega_m\\ -1 & 1\\ \omega_n & \omega_m\end{pmatrix}\begin{Bmatrix}\xi_m\\ \zeta_n\end{Bmatrix}\qquad(19)$$

Thus, the equation for forced vibration now may be evaluated as:

$$\left[K_g\right]\{\Delta\}+\left[C_g\right]\{\dot{\Delta}\}+\left[M_g\right]\{\ddot{\Delta}\}=\{F_t\}\qquad(20)$$

Where $\{F_t\}$ is time-varying loading; $\{\Delta\}$ is displacement at time t; ω is the frequency of vibration and λ is the Eigenvector and its derivatives for velocity and acceleration. The dynamic response analysis was carried by using Newmark-β technique.

Fig 1. shows the plan view of a laminated composite skew plate with the skew angle as α. The necessary skew

transformation was carried out by using the transformation matrix below.

$$[T]=\begin{pmatrix} c & -s & 0 & 0 & 0 & 0 & 0 \\ s & c & 0 & 0 & 0 & 0 & 0 \\ 0 & 0 & 1 & 0 & 0 & 0 & 0 \\ 0 & 0 & 0 & c & -s & 0 & 0 \\ 0 & 0 & 0 & s & c & 0 & 0 \\ 0 & 0 & 0 & 0 & 0 & c & -s \\ 0 & 0 & 0 & 0 & 0 & s & c \end{pmatrix}, \text{where } c=\cos\alpha \text{ and } s=\sin\alpha$$

2.2 Boundary condition

The boundary/support condition considered in the present study was simply supported at all four edges (SSSS).

SSSS:

$u_2 = u_3 = \Psi_2 = w_2 = 0$ at $x = 0, a$ and

$u_1 = u_3 = \Psi_1 = w_1 = 0$ at $y = 0, b$

3. Numerical application and results

In the present study, many novel problems on forced vibration of laminated composite plates were solved by using the present FE model and mathematical formulation (ISDT).

3.1 Engineering and geometrical properties

In all the further investigations, unless mentioned otherwise, the engineering properties for laminated composite plates were taken as given in Table 1.

The geometrical properties taken into consideration were:

The total thickness of the plate (h) = 3.81 cm

The length of the plate: a= b=20 h.

Table 1 Material properties of the laminated composite plate

$\mathbf{E_1}$ (GPa)	$\mathbf{E_2}$ (GPa)	$\mathbf{G_{12}}$ (GPa)	$\mathbf{G_{13}}$ (GPa)	$\boldsymbol{\mu_{12}}$	ρ(kN/m^3)
172.369	6.895	3.448	3.448	0.25	1603.03

3.2 Applied loads

The different types of loadings in the spatial and time domain are:

$$q = q_0 \sin\left(\frac{\pi x}{a}\right)\sin\left(\frac{\pi y}{b}\right)F(t)$$

$$q = q_0 \cos\left(\frac{\pi x}{a}\right)\sin\left(\frac{\pi y}{b}\right)F(t)$$

$$q = q_0 \cos\left(\frac{\pi x}{a}\right)\cos\left(\frac{\pi y}{b}\right)F(t)$$

where,

$F(t) = \{1, 0 \geq t\}$: Rectangular step pulse

$F(t) = \begin{Bmatrix} 1, & 0 \leq t \leq t_1 \\ 0, & t > t_1 \end{Bmatrix}$: Rectangular pulse

$F(t) = \begin{Bmatrix} t/t_1, & 0 \leq t \leq t_1 \\ 0, & t > t_1 \end{Bmatrix}$: Triangular pulse loading (I)

$F(t) = \begin{Bmatrix} 1 - t/t_1, & 0 \leq t \leq t_1 \\ 0, & t > t_1 \end{Bmatrix}$: Triangular pulse loading (II)

$F(t) = \begin{Bmatrix} \sin(\pi t/t_1), & 0 \leq t \leq t_1 \\ 0, & t > t_1 \end{Bmatrix}$: Sine pulse loading

The non-dimensional stresses as follows:

$$q = q_0 \sin\left(\frac{\pi x}{a}\right)\sin\left(\frac{\pi y}{b}\right)F(t)$$

$$q = q_0 \cos\left(\frac{\pi x}{a}\right)\sin\left(\frac{\pi y}{b}\right)F(t)$$

$$q = q_0 \cos\left(\frac{\pi x}{a}\right)\cos\left(\frac{\pi y}{b}\right)F(t)$$

$$\bar{\sigma}_{xx} = \sigma_{xx}\left(\frac{a}{2}, \frac{b}{2}, \frac{h}{2}\right)/100q_0$$

$$\bar{\sigma}_{yy} = \sigma_{yy}\left(\frac{a}{2}, \frac{b}{2}, z\right)/100q_0$$

$$\bar{\sigma}_{xy} = \sigma_{xy}\left(0, 0, -\frac{h}{2}\right)/100q_0$$

3.2 Convergence and validation study

The convergence study was carried out and the results were found to converge at 20 x 20 mesh size. Hence, all results were computed at 20 x 20 mesh size.

For validation study, the problem solved earlier by (Wang *et al*. 2001) was taken into consideration. In this example, a three-layer cross-ply (0°/90°/0°) square laminated plate is considered. The engineering and geometrical properties were taken as discussed in the earlier section. The load was sinusoidally distributed over the whole surface of the plate which varies with time. The expression is given below:

$$q = q_0 \cos\left(\frac{\pi x}{a}\right)\sin\left(\frac{\pi y}{b}\right)F(t)$$

where

$F(t) = \begin{Bmatrix} 1, & 0 \leq t \leq t_1 \\ 0, & t > t_1 \end{Bmatrix}$: Rectangular pulse

In Table 2 and 3, the results for deflection and stresses of laminated composite plates were compared with the published literature. The variation of the result is the reason why (Wang *et al*. 2001) used CLPT and the present results are based upon the suitable ISDT that includes the effect of transverse shear and rotary inertia.

Further comparison study for skew laminated composite plates was carried out in Table 4. The problem of a rectangular laminate subjected to uniformly distributed

Table 2 Validation of maximum deflection of laminated composite plate with lamination (0°/90°/0°)

	For a/h = 20		
Type of pulse	Rectangular	Triangular	Sine
Present	2.9672	2.5602	1.9102
(Wang *et al*. 2001)	2.6666	2.3071	1.6818

Table 3 Validation of maximum stress ($\bar{\sigma}_{xx}$) of laminated composite plate with lamination (0°/90°/0°)

	For a/h=20
Type of pulse	Rectangular Pulse
Present	443.532
(Wang *et al*. 2001)	440.909

Table 4 Non-dimensional central deflections of a laminated composite skew plate subjected to uniformly distributed loading (b/a=1) for laminate (0°/90°/0°) composite skew plate for skew angle (α)

		α			
a/h	References	0	15	30	45
10	Present (20×20)	10.9812	10.4300	8.6613	5.7181
	(Sheikh and Chakrabarti 2003)	10.9117	10.3669	8.6217	5.7105

loading as solved by (Sheikh and Chakrabarti 2003) using HSDT was considered in this example. The deflection presented in Table 4 were found to be in good coherence with the results of (Sheikh and Chakrabarti 2003).

4. Novel results

After validation studies, many new examples were solved for dynamic analysis of laminated composite skew plate under different types of spatial and transient loads. For all calculations, 20×20 mesh size was used. In the following examples, each lamina of the laminated plate has the same thicknesses and material properties. The time step (*dt*) was taken as 0.03 μ second for all further calculations.

Example (1) A two-layer cross-ply (0°/90°) laminated composite skew plate was considered. The engineering and geometrical properties were taken as discussed in the earlier section.

The finishing time of pulse (t) =0.006 second was taken. The intensity of the transverse load was taken to be q_0 = 3.448 MPa. The boundary condition was all edges simply supported and skew angles were 0°, 15°, 30°, 45° and 60°.

The load considered was time varying sinusoidally distributed on the whole surface of the plate and was given as:

$$q = q_0 \sin\left(\frac{\pi x}{a}\right)\sin\left(\frac{\pi y}{b}\right)F(t)$$

where

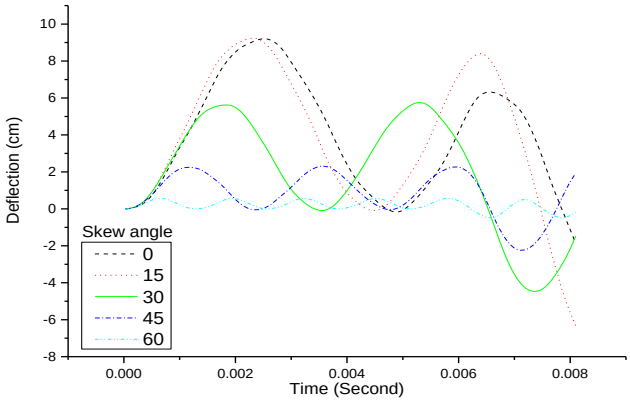

Fig. 3. Deflection history of the laminated composite skew plate (0°/90°) under rectangular pulse

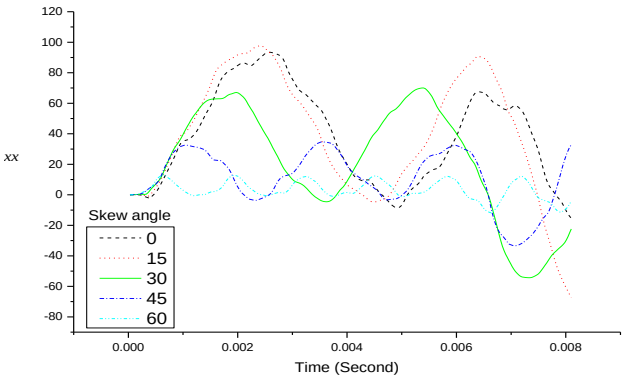

Fig. 4. Non-dimensional stress ($\bar{\sigma}_{xx}$) history of the laminated composite skew plate (0°/90°) under rectangular pulse

$$F(t) = \begin{Bmatrix} 1, & 0 \le t \le t_1 \\ 0, & t > t_1 \end{Bmatrix}: \qquad \text{Rectangular pulse}$$

In order to check the behaviour of the laminated composite plate under various skew angles, the analysis was carried out with variation in the skew angles at a particular boundary condition. The results in form of deflection and stresses were shown in Figs. 3-4. In Fig. 3 the deflection history is plotted for the various skew angles of the laminated composite plate. In the Figure, it can be observed that the 0° and 15° skew plate show the maximum deflection of about 9 cm whereas the 60° skew plate shows the lowest deflection of about 0.7 cm. According to the Figure, the reduction of deflection is observed for an increase in skew angle from 0° to 60°.

In Fig. 4, the variation of non-dimensional stress $\bar{\sigma}_{xx}$ with respect to time is plotted for the various laminated composite skew plate. In the figure, the 15° skew composite plate shows maximum stress whereas, the 60° skew composite plate shows the minimum stress.

Example (2) A three-layer cross-ply (0°/90°/0°) laminated composite skew plate was considered. The engineering and geometrical properties were taken as discussed in the earlier section.

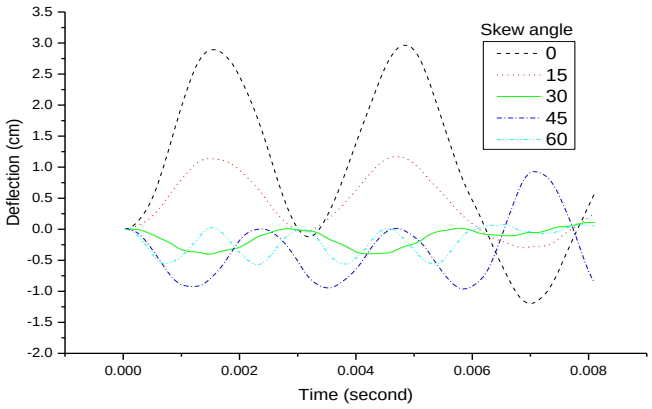

Fig. 5. Deflection history of the laminated composite skew plate (0°/90°/0°) under rectangular pulse

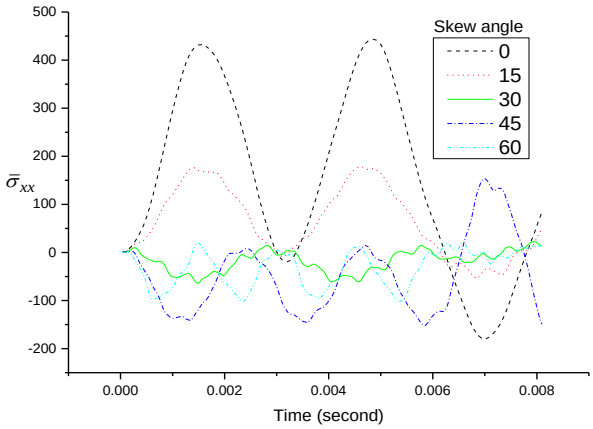

Fig. 6. Non-dimensional stress ($\bar{\sigma}_{xx}$) history of the laminated composite skew plate (0°/90°/0°) under rectangular pulse

The finishing time of pulse (t) =0.006 second was taken. The intensity of the transverse load was taken to be q_0 =3.448 MPa. The boundary condition was all edges simply supported and skew angles were 0°, 15°, 30°, 45° and 60°.

The considered load was time varying sinusoidally distributed on the whole surface of the plate and was given as:

$$q = q_0 \sin\left(\frac{\pi x}{a}\right)\sin\left(\frac{\pi y}{b}\right)F(t)$$

where

$$F(t) = \begin{Bmatrix} 1, & 0 \le t \le t_1 \\ 0, & t > t_1 \end{Bmatrix} : \quad \text{Rectangular pulse}$$

In Figure 5, the deflection history is plotted. According to the figure, it was observed that 0° skew laminated composite plate had maximum amplitude of deflections as compared to other skew angles i.e. almost 3 cm and for other skew angles, i.e. 30°, 45° and 60° amplitude of deflections was less than 1 cm.

In Fig. 6, the non-dimensional stress ($\bar{\sigma}_{xx}$) history is plotted. The figure, indicates that the 0° skew laminated composite plate shows the highest amplitude whereas, the

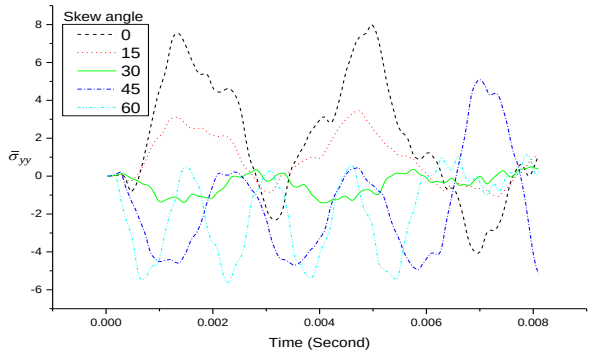

Fig. 7. Non-dimensional stress ($\bar{\sigma}_{yy}$) history of the laminated composite skew plate (0°/90°/0°) under rectangular pulse

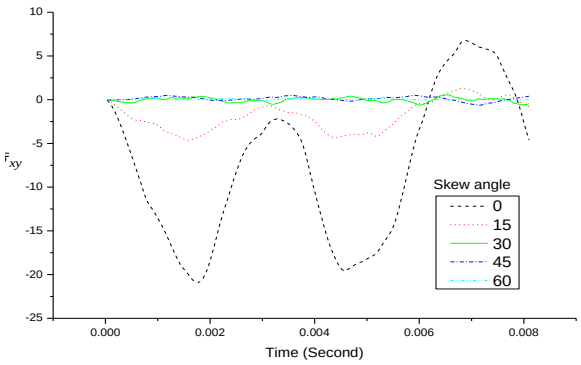

Fig. 8. Non-dimensional stress ($\bar{\sigma}_{xy}$) history of the laminated composite skew plate (0°/90°/0°) under rectangular pulse

lowest amplitude is for the 30° and 60° skew angles of the laminated composite plate.

In Fig. 7, the non-dimensional stress ($\bar{\sigma}_{yy}$) history is plotted. The figure shows that the highest amplitude with a maximum peak value of about 8 was observed for the 0° skew plate, whereas the 30° skew plate showed the lowest amplitude having a maximum peak value of about 0.5.

In Fig. 8, the non-dimensional stress ($\bar{\sigma}_{xy}$) history is plotted. From the figure, it is observed for the 0° skew plate have the highest amplitude with a maximum peak value of about 6.5 whereas the lowest amplitude with maximum peak value for the 60° skew plate i.e. 0.1.

Example (3) A four-layer cross-ply (0°/90°/0°/90°) laminated composite skew plate is considered. The engineering and geometrical properties were taken as discussed in the earlier section.

The finishing time of pulse (t) =0.006 second was taken. The intensity of the transverse load was taken to be q_0 = 3.448 MPa. The boundary condition was all edges simply supported and skew angles were 0°, 15°, 30°, 45° and 60°.

The load considered was time varying sinusoidally distributed on the whole surface of the plate and was given as:

$$q = q_0 \sin\left(\frac{\pi x}{a}\right)\sin\left(\frac{\pi y}{b}\right)F(t)$$

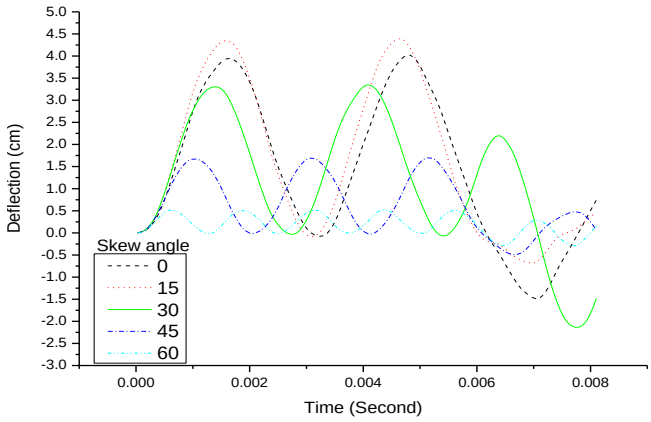

Fig. 9. Deflection history of the laminated composite skew plate (0°/90°/0°/90°) under rectangular pulse

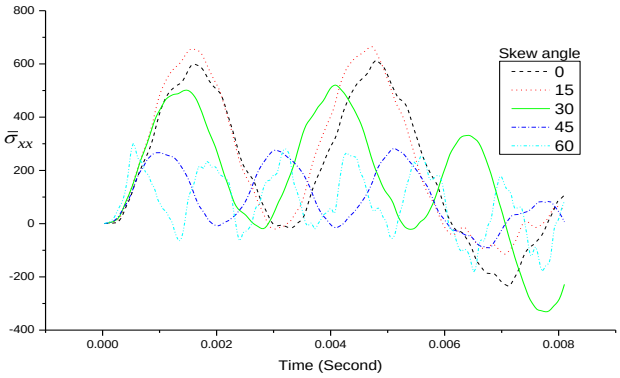

Fig. 10. Non-dimensional stress $(\bar{\sigma}_{xx})$ history of the laminated composite skew plate (0°/90°/0°/90°) under rectangular pulse

where

$$F(t)=\begin{Bmatrix}1, & 0\le t\le t_1\\ 0, & t>t_1\end{Bmatrix}: \quad \text{Rectangular pulse}$$

Figure 9-12, shows the variation of deflection and stresses for the laminated composite skew plate. Fig. 9 shows the deflection history. The figure indicates that the 15° skew plate shows a maximum deflection of about 4.4 cm, whereas 0°and 30° skew plate shows a maximum deflection of about 3.2 cm. The 60° skew plate shows the lowest deflection of about 0.5 cm.

Fig. 10 shows the non-dimensional stress $(\bar{\sigma}_{xx})$ history. From the figure, it is observed that the 15° skew plate shows the maximum stress of about 680, whereas the 0° skew plate shows the stress of about 600.

Fig. 11 shows the non-dimensional stress $(\bar{\sigma}_{yy})$ history. The figure indicates that the 15° skew plate shows the maximum stress of about 360. It is also concluded that $(\bar{\sigma}_{yy})$ stresses are lower as compared to the $(\bar{\sigma}_{xx})$ stresses.

Fig. 12 shows the non-dimensional stress $(\bar{\sigma}_{xy})$ history. From the figure, it is observed that the 0° skew plate shows the maximum stress of about 8. It is also concluded that the $(\bar{\sigma}_{xy})$ amplitude of stresses is lower than for the $(\bar{\sigma}_{xx})$ and $(\bar{\sigma}_{yy})$ stresses. According to the figures, the deflections and

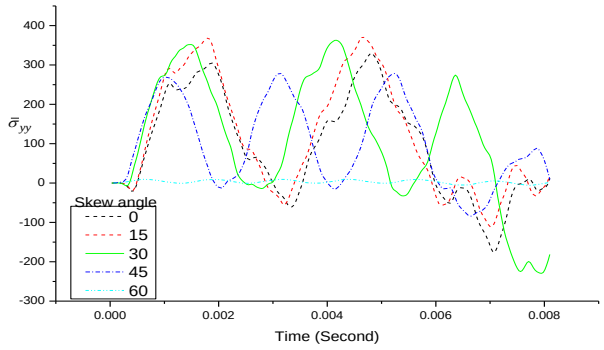

Fig. 11. Non-dimensional stress $(\bar{\sigma}_{yy})$ history of the laminated composite skew plate (0°/90°/0°/90°) under rectangular pulse

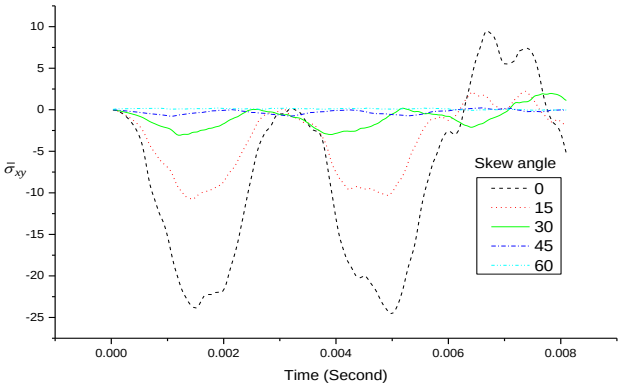

Fig. 12. Non-dimensional stress $(\bar{\sigma}_{xy})$ history of the laminated composite skew plate (0°/90°/0°/90°) under rectangular pulse

non-dimensional stresses peak value for four-layer cross-ply laminates are higher as compared to two and three-layered laminates.

Example (4) A five-layer cross-ply (60°/-30°/0°/-30°/60°) laminated composite skew plate was considered. The engineering and geometrical properties were taken as discussed in the earlier section.

The finishing time of pulse (t) =0.006 second was taken. The intensity of the transverse load was taken to be q_0 = 3.448 MPa. The boundary condition was all edges simply supported and skew angles were 0°, 15°, 30°, 45° and 60°.

The load considered was time varying sinusoidally distributed on the whole surface of the plate and was given as:

$$q=q_0\sin\left(\frac{\pi x}{a}\right)\sin\left(\frac{\pi y}{b}\right)F(t)$$

where

$$F(t)=\begin{Bmatrix}1, & 0\le t\le t_1\\ 0, & t>t_1\end{Bmatrix}: \quad \text{Rectangular pulse}$$

Figs. 13-15 show the deflection and stresses history for the five-layer cross-ply laminated composite plate. Fig. 13 shows the deflection history. From the figure, it is observed that the 15° skew composite plate shows a maximum

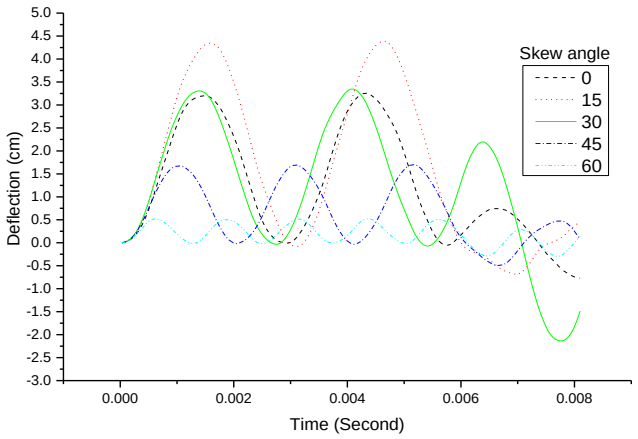

Fig. 13. Deflection history of the laminated composite skew plate (60°/-30°/0°/-30°/60°) under rectangular pulse.

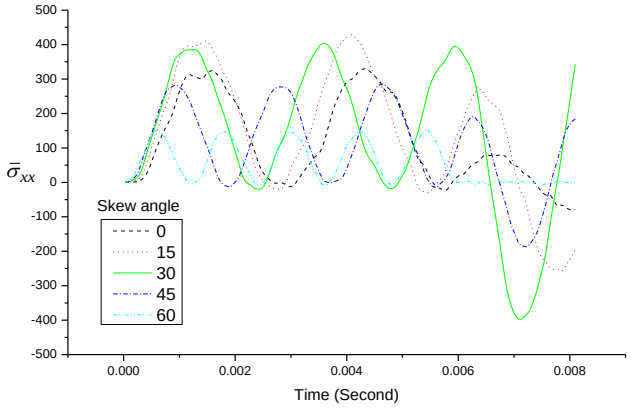

Fig. 14. Non-dimensional stress ($\bar{\sigma}_{xx}$) history of the laminated composite skew plate (60°/-30°/0°/-30°/60°) under rectangular pulse

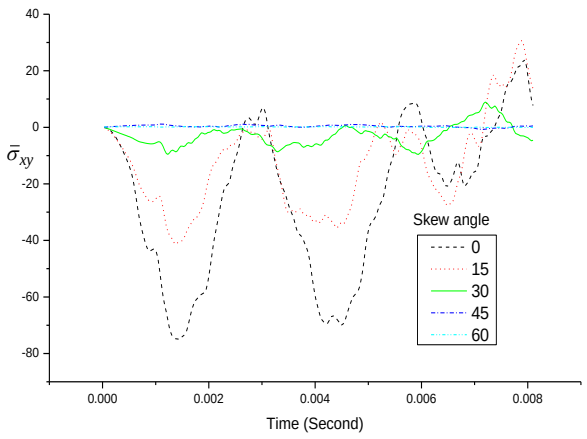

Fig. 15. Non-dimensional stress ($\bar{\sigma}_{xy}$) history of the laminated composite skew plate (60°/-30°/0°/-30°/60°) under rectangular pulse.

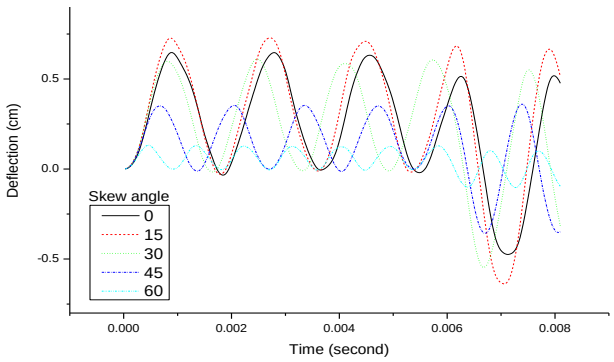

Fig. 16. Deflection history of the laminated composite skew plate (0°/90°/0°) under rectangular pulse, h/a=0.1

deflection of about 4.5 cm, whereas the 30° plate shows 3.3 cm. It was also observed that the 60° skew plate shows the lowest deflection of about 0.4 cm.

Fig. 14 shows the non-dimensional stress ($\bar{\sigma}_{xx}$) history. From the figure, it is observed that the 15° skew plate shows the maximum stress of about 425, whereas the 60° skew plate shows the lowest stress of about 150.

Fig. 15 shows the non-dimensional stress ($\bar{\sigma}_{xy}$) history. The figure indicates that the amplitude variation for ($\bar{\sigma}_{xy}$) stresses of 0° and 15° skew plates shows negative values whereas the other skew plate shows a linear variation of amplitude.

Example (5) A three-layer cross-ply (0°/90°/0°) laminated composite skew plate was considered. The engineering properties were taken as in Table 1 and the geometrical properties were a = b = 0.762m, h/a ratio= 0.1 and 0.2. The finishing time of pulse (t) =0.006 second was taken. The intensity of the transverse load was taken to be q_0 = 3.448 MPa. The boundary condition was all edges simply supported and skew angles were 0°, 15°, 30°, 45° and 60°.

The load considered was time varying sinusoidally, distributed on the whole surface of the plate and was given as:

$$q = q_0 \sin\left(\frac{\pi x}{a}\right)\sin\left(\frac{\pi y}{b}\right)F(t)$$

where

$$F(t) = \begin{Bmatrix} 1, & 0 \le t \le t_1 \\ 0, & t > t_1 \end{Bmatrix} : \quad \text{(Rectangular pulse)}$$

In the example, two thickness ratios were taken to check the dynamic behaviour of a laminated composite plate having different skew angles. The variations of deflection and stresses were shown in Fig. 16-19 for different skew angles of the laminated plate. The thickness ratio was taken as 0.1.

Fig. 16 shows the deflection history. From the figure, it was observed that the maximum peak value is about 0.7 of 15° skew laminated plate. For the 0° skew plate, the amplitude is quite lower than 15° and the maximum peak value is about 0.6. The minimum amplitude of the maximum peak value is for the 60° skew plate that is about 0.1. The reason for the reduced maximum peak values of deflection is accounted for in the low value of the thickness of the plate.

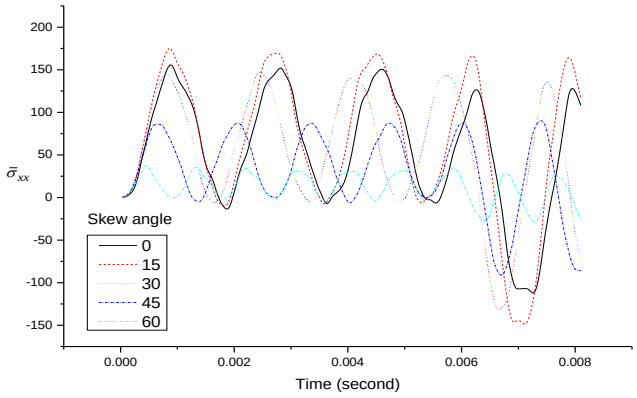

Fig. 17. Non-dimensional stress $(\bar{\sigma}_{xx})$ history of the laminated composite skew plate (0°/90°/0°) and h/a=0.1

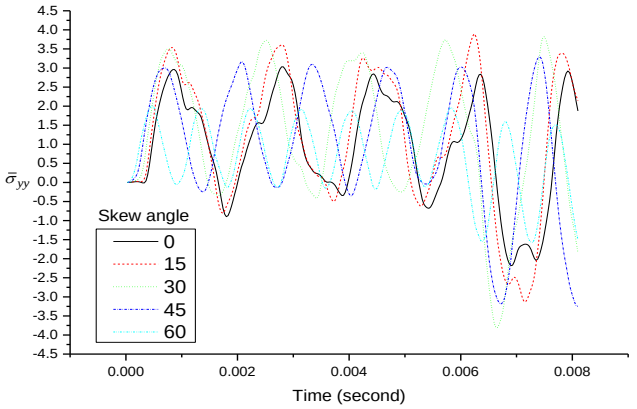

Fig. 18. Non-dimensional stress $(\bar{\sigma}_{yy})$ history of the laminated composite skew plate (0°/90°/0°) and h/a=0.1

Fig. 17 shows the non-dimensional stress $(\bar{\sigma}_{xx})$ history. From the figure, it is concluded that the 15° skew plate has the highest amplitude with maximum peak value as 175 whereas, for the 45° and 60° plates the amplitude was lower than others, having maximum peak value of 90 and 35, respectively.

Fig. 18 shows the non-dimensional stress $(\bar{\sigma}_{yy})$ history. From the figure, it is observed that the 0° skew plate has the highest amplitude with maximum peak value as 3. This non-dimensional stress value is very low, as compared to $(\bar{\sigma}_{xx})$. The 60° skew plates have the minimum amplitude than 0°, 30° and 45° plates.

Fig. 19 shows the non-dimensional stress $(\bar{\sigma}_{xy})$ history. The figure indicates that the highest amplitude with a maximum peak value of 6 is for 0° skew plate, whereas the lowest amplitude with maximum peak value is about 0.1 for the 60° skew laminated plate.

The variation of deflection and stresses were shown in Fig. 20-23 for different skew angles of the laminated plate. The thickness ratio was taken as 0.2.

Fig. 20 shows the non-dimensional deflection history. From the figure, it is concluded that the highest amplitude with maximum peak value is about 0.16 of the 15° skew plate, whereas the 60° skew plate shows the lowest

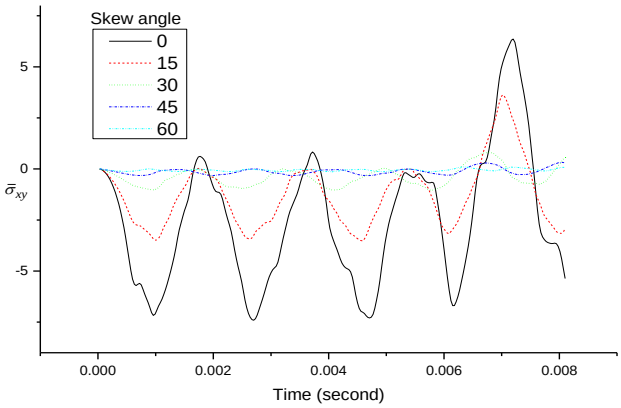

Fig. 19. Non-dimensional stress $(\bar{\sigma}_{xy})$ history of the laminated composite skew plate (0°/90°/0°) and h/a=0.1

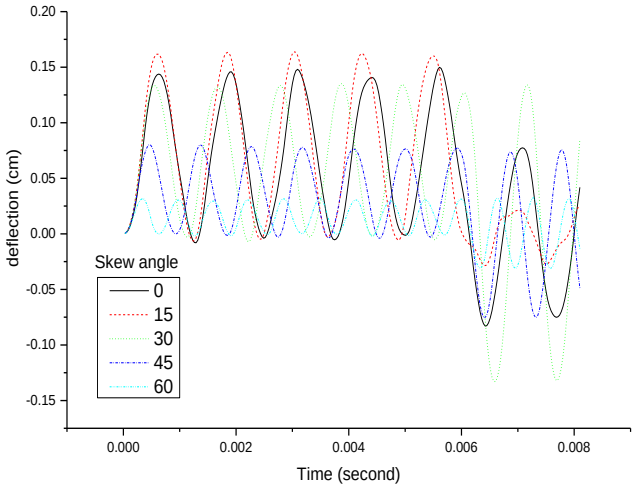

Fig. 20. Deflection history of the laminated composite skew plate (0°/90°/0°) and h/a=0.2

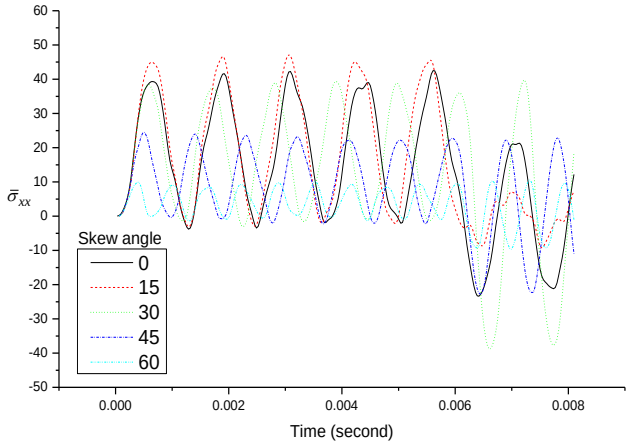

Fig. 21. Non-dimensional stress $(\bar{\sigma}_{xx})$ history of the laminated composite skew plate (0°/90°/0°) and h/a=0.2

amplitude with peak value as 0.03 cm for 0.2 thickness ratio.

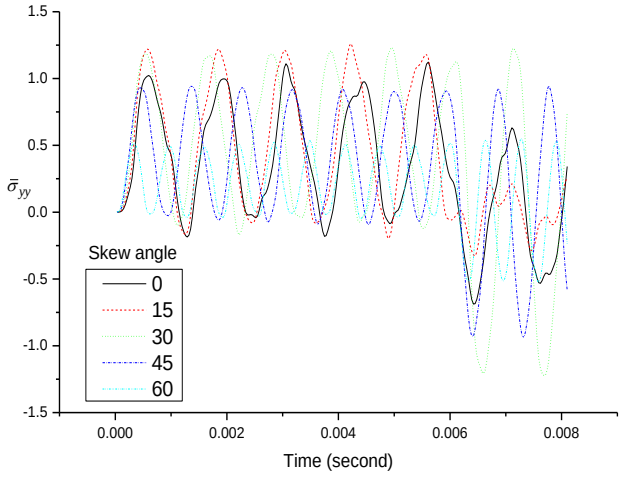

Fig. 22. Non-dimensional stress ($\bar{\sigma}_{yy}$) history of the laminated composite skew plate (0°/90°/0°) and h/a=0.2

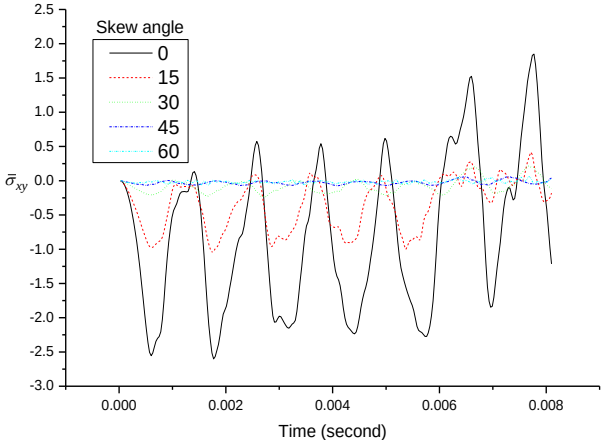

Fig. 23. Non-dimensional stress ($\bar{\sigma}_{xy}$) history of the laminated composite skew plate (0°/90°/0°) and h/a=0.2

Fig. 21 shows the non-dimensional stress ($\bar{\sigma}_{xx}$) history. From the figure, it is seen that the 15° skew plate has the highest amplitude with a maximum peak value of whereas the lowest value is for the 60° skew laminated plate of 10.

Fig. 22 shows the non-dimensional stress ($\bar{\sigma}_{yy}$) history. The figure indicates that the 15° skew plate has the highest amplitude with maximum peak value as 1.2 whereas the lowest amplitude is for the 60° skew plate, i.e. 0.5 cm.

Fig. 23 shows the non-dimensional stress ($\bar{\sigma}_{xy}$) history. From the figure, it is concluded that the highest amplitude and a maximum peak value of about 1.84 are observed for the 0° skew plate, whereas the lowest amplitude with a peak value of 0.05 is for the 45° and 60° skew laminated plates.

It was also concluded that in order to reduce the deflection or stresses of laminated composite plates, the increase in the thickness ratio of the plate is required.

5. Conclusions

- A 2D FE model was developed using mathematical formulation based upon cubic variation of thickness coordinate in displacement fields including skew transformations for transient analysis of laminated composite skew plate.
- The present 2D FE model predicts results close to the analytical results.
- (0°/90°) the laminated composite plate shows maximum deflection and low stress as compared to other considered lamination schemes.
- Deflection and in-plane stresses for the 0° and 15° skew laminated plates are higher than for other skew angles i.e. 30°,45° and 60°.
- With the increase in the thickness of the laminated plate, reduction of deflection and in-plane stresses occur.
- Numerical results of the transient response of rhombic laminates based on present formulation will serve as a point of reference for future scholars. It will also help construction industry and engineers in the selection of proper laminates.

The forced vibration of laminated composite plates using ISDT was carried for the first time. The present 2D FE C^0 model solutions are in good agreement with the analytical solutions and hence, useful enough to explore the effect of the dynamic behaviour of laminated composite twisted plates.

References

Adim, B., Daouadji, T.H. and Rabahi, A. (2016), "A simple higher order shear deformation theory for mechanical behavior of laminated composite plates", *J. Adv. Struct. Eng. (IJASE)*, Springer Berlin Heidelberg, **8**(2), 103-117.

Ahmadian, M.T. and Zangeneh, M.S. (2003), "Forced vibration analysis of laminated rectangular plates using super elements", *Scientia Iranica*, **10**(2), 260-265.

Ahmed, J.K., Agarwal, V.C., Pal, P. and Srivastav, V. (2013), "Static and dynamic analysis of composite laminated plate", *J. Innovative Technol. Explor. Eng.*, **3**(6), 56-60.

Akbarov, S.D. and Mehdiyev, M.A. (2017), "Forced vibration of the elastic system consisting of the hollow cylinder and surrounding elastic medium under perfect and imperfect contact", *Struct. Eng. Mech.*, **62**(1), 113-123.

Bathe, K.J. (1996), *Finite Element Method. Wiley Encyclopedia of Computer Science and Engineering*, John Wiley & Sons, Inc., Hoboken, NJ, USA.

Campbell, F.C. (2003), *Manufacturing Processes for Advanced Composites*, Elsevier Science, Netherlands.

Chamis, C.C. (2006), "Probabilistic design of composite structures", NASA/TM-2006-214660; NASA Glenn Research Center; Cleveland, OH, USA.

Dambal, S.V. and Sharma, R.S. (2013), "Finite element simulation of transient response analysis of woven glass/epoxy laminated plates", *J. Res. Aeronaut. Mech. Eng.*, **13**, 44-51.

Golewski, G.L. (2017), "Determination of fracture toughness in concretes containing siliceous fly ash during mode III loading", *Struct. Eng. Mech.*, **62**(1), 1-9. https://doi.org/10.12989/sem.2017.62.1.001.

Golewski, G.L. (2018a), "An assessment of microcracks in the Interfacial Transition Zone of durable concrete composites with fly ash additives", *Compos. Struct.*, **200**, 515. https://doi.org/10.1016/j.compstruct.2018.05.144.

Golewski, G.L. (2018b), "Evaluation of morphology and size of cracks of the Interfacial Transition Zone (ITZ) in concrete containing fly ash (FA)", *J. Hazardous Mater.*, **357**, 298.

Hoa, S.V. and Xiao, X. (1998), "A new rectangular plate element for vibration analysis of laminated composites", *J. Vib. Acoustics*, **120**(1), 81. https://doi.org/10.1115/1.2893830.

Kant, T., Arora, C.P. and Varaiya, J.H. (1992), "Finite element transient analysis of composite and sandwich plates based on a refined theory and a mode superposition method", *Compos. Struct.*, **22**(2), 109-120. https://doi.org/10.1016/0263-8223(92)90071-J.

Kiral, Z. and Kiral, B.G. (2008), "Dynamic analysis of a symmetric laminated composite beam subjected to a moving load with constant velocity", *J. Reinforced Plastics Compos.*, **27**(1), 19-32. https://doi.org/10.1177/0731684407079492.

Lee, S.J. and Kim, H.R. (2013), "FE analysis of laminated composite plates using a higher order shear deformation theory with assumed strains", *Latin J. Solid Struct.*, **10**(3), 523-547. https://doi.org/10.1002/nme.1620211207.

Maithry, K., Chandra, D.V, and Rao, M. (2012), "Dynamic analysis of laminated composite plates with holes", *J. Res. Eng. Tech.*, **4**(May), 116-121.

Mallikarjuna, and Kant, T. (1988), "Dynamics of laminated composite plates with a higher order theory and finite element discretization", *J. Sound Vib.*, **126**(3), 463-475.

Mantari, J.L., Oktem, A.S. and Guedes Soares, C. (2012), "Bending response of functionally graded plates by using a new higher order shear deformation theory", *Compos. Struct.*, **94**(2), 714-723. https://doi.org/10.1016/j.compstruct.2011.09.007.

Patel, B.P., Gupta, S.S., Joshi, M. and Ganapathi, M. (2005), "Transient response analysis of bimodulus anisotropic laminated composite plates", *J. Reinforced Plastics Compos.*, **24**(8), 795-821. https://doi.org/10.1177/0731684405047768.

Reddy, J.N. (1983), "Dynamic (transient) analysis of layered anisotropic composite-material plates", *J. Numeric. Methods Eng.*, **19**(2), 237-255. https://doi.org/10.1002/nme.1620190206.

Sheikh, A.H. and Chakrabarti, A. (2003), "A new plate bending element based on higher-order shear deformation theory for the analysis of composite plates", *Finite Elements Anal. Design*, **39**(9), 883-903. https://doi.org/10.1016/S0168-874X(02)00137-3.

Shooshtari, A. and Khadem, S.E. (2006), "A multiple scales method solution for the free and Forced nonlinear transverse vibrations of rectangular plates", *Struct. Eng. Mech.*, **24**(5), 543-560. https://doi.org/10.12989/sem.2006.24.5.543.

Sun, C. and Whitney, J.M. (1974), "Forced vibrations of laminated composite plates in cylindrical bending", *J. Acoustic. Soc. America*, Acoustical Society of America, **55**(5), 1003-1008. https://doi.org/10.1121/1.1914639.

Tahani, M. and Torghabeh, I.G. (2011), "Transient analysis of rectangular laminated plates subjected to dynamic transverse loading using a layerwise theory", *10th WSEAS International Conference on Applied Computer and Applied Computational Science*, Venice, Italy, March.

Wang, Y.Y., Lam, K.Y. and Liu, G.R. (2001), "A strip element method for the transient analysis of symmetric laminated plates", *J. Solids Struct.*, **38**(2), 241-259. https://doi.org/10.1016/S0020-7683(00)00035-4.

Yousefi, P., Hosseini-Hashemi, S. and Kargarnovin, M.H. (2012), "Force vibration of laminated plates with various shapes subjected to low-velocity impact", *J. Mater. Sci. Res.*, **1**(3), 106. http://doi.org/10.5539/jmsr.v1n3p106.